JOURNAL OF MATERIALS SCIENCE **40** (2005) 1577– 1582

High temperature compressive properties over a wide range of strain rates in an AZ31 magnesium alloy

K. ISHIKAWA*, H. WATANABE
Osaka Municipal Technical Research Institute, 1–6–50 Morinomiya, Joto-ku, Osaka 536–8553, Japan
E-mail: isikawak@omtri.city.osaka.jp

T. MUKAI
Research Center for Advanced Science and Technology, The University of Tokyo, 4–6–1 Komaba, Meguro-ku, Tokyo 153-8904, Japan

High temperature compressive properties in AZ31 magnesium alloy were examined over a wide strain rate range from 10^{-3} to 10^{3} s^{-1}. It was suggested that the dominant deformation mechanism in the low strain rate range below 10^{-1} s^{-1} was dislocation creep controlled by pipe diffusion at low temperatures, and by lattice diffusion at high temperatures. On the other hand, analysis of the flow behavior and microstructural observations indicated that the deformation at high strain rates of $\sim 10^{3}$ s^{-1} proceeds by conventional plastic flow of dislocation glide and twinning even at elevated temperatures.

1. Introduction

Die casting has been a principal technique for the fabrication of magnesium components because of its high productivity, suitable strength, quality and dimensional control [1–3]. The fabrication is also performed by semi-solid processing of thixotropic molding [1, 4]. However, the fabrication by plastic forming also has considerable potential because the alloys have higher ductility and strength than the castings [3, 5, 6], and because plastic forming enables high productivity and superior mechanical properties. It is expected that processes utilizing plastic forming will be developed.

Plastic formability of magnesium alloys is enhanced at elevated temperatures, because non-basal slips are activated in addition to basal slip [7], or superplasticity is observed in fine-grained magnesium alloys [8, 9]. At present, plastic forming of AZ31 magnesium alloy by deep drawing [10] or forging [11] has been adopted as a secondary processing in fabricating several electric appliance housings. In order to optimize the processing for plastic forming, it is important to understand the effect of temperature and strain rate on flow stress. To date, high temperature deformation behavior [12–28] or hot working characteristics [17, 19, 24, 25, 27, 29–31] of AZ31 alloy has been examined extensively. However, deformation behavior at high strain rates of $1–10^{3}$ s^{-1}, where the plastic forming may be performed [32], has rarely been investigated even in magnesium alloys [33–38]. Therefore, in the present study, high temperature deformation behavior of AZ31 alloy was examined by compression tests over a wide strain rate range from 10^{-3} to 10^{3} s^{-1} with emphasis on the behavior at high strain rates. The deformation behavior was analyzed in connection with the operating deformation mechanism.

2. Experimental

The alloy used in the present study was a commercial Mg–Al–Zn alloy, AZ31. The material was received as an ingot. The material was solution treated at a temperature of 686 K for 48 h followed by water quenching. The grain size of the solution treated material was 150 μm.

Cylindrical specimens of diameter 10 mm and height 5 mm were used for compression tests. The compression tests were carried out at temperatures ranging from 296 to 723 K and at strain rates from 10^{-3} to 10^{3} s^{-1} in air. The compression tests at strain rates below 10^{-1} s^{-1} and at a high strain rate of 10^{3} s^{-1} were performed using Instron testing machine and a Hopkinson pressure bar, respectively. The deformed specimens were water cooled, sectioned parallel to the compression axis, and examined using standard metallographic techniques.

Dynamic shear modulus, G, was measured from room temperature to 693 K by employing the method of resonant vibration in cantilever specimen holding, except at room temperature, which were performed by the free resonance vibrations. The specimen had a rectangular shape with the length of 60 mm, width of 10 mm

*Author to whom all correspondence should be addressed.

and thickness of 1.5 mm. The specimen was prepared by machining.

3. Results

The true stress–true strain curves up to true strain of 0.2 are shown in Fig. 1 for materials deformed at (a) $\dot{\varepsilon} \approx 10^{-3}$ s^{-1} and (b) $\dot{\varepsilon} \approx 10^{3}$ s^{-1}. When the material was deformed at above 573 K and at 10^{-3} s^{-1}, steady state flow region was observed over the wide strains. On the other hand, strain hardening was observed at all temperatures when the material was deformed at a high strain rate of 10^{3} s^{-1}, and it was significant especially at room temperature. The effect of deformation temperature on flow stress was relatively small at a high strain rate.

The variation in flow stress as a function of deformation temperature is shown in Fig. 2 for all strain rates examined. The flow stress for each strain rate was determined at a fixed strain of 0.1. It is obvious that the flow stress monotonically decreased with temperature.

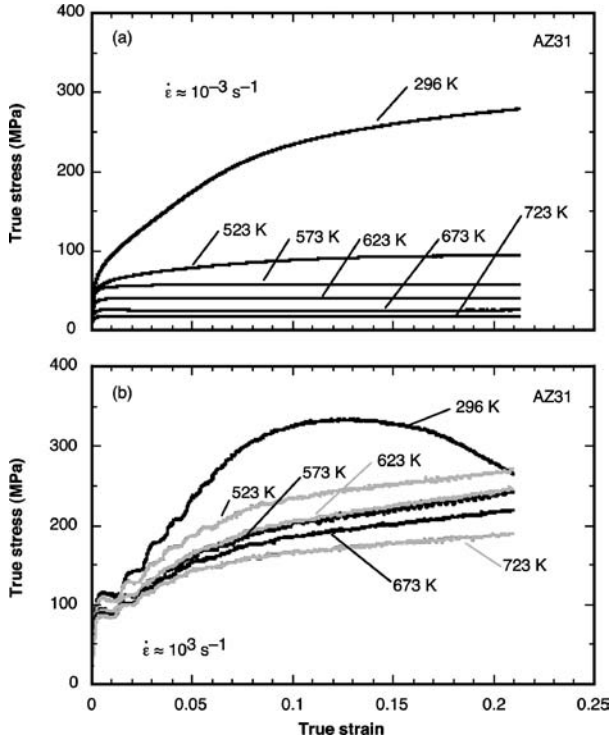

Figure 1 True stress—true strain curves up to true strain of 0.2 in AZ31 deformed at various temperatures and at (a) $\dot{\varepsilon} \approx 10^{-3}$ s^{-1} and (b) $\dot{\varepsilon} \approx 10^{3}$ s^{-1}.

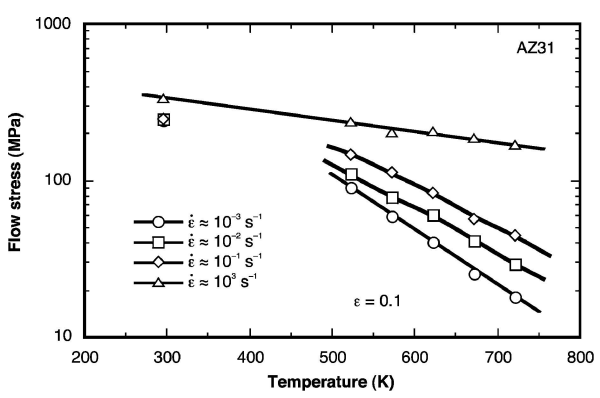

Figure 2 The variation in flow stress as a function of deformation temperature at various strain rates.

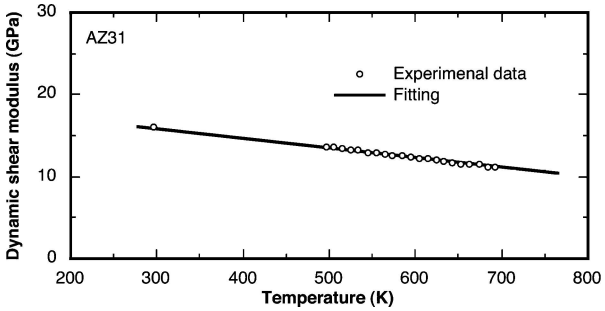

Figure 3 The variation in shear modulus as a function of temperature for AZ31.

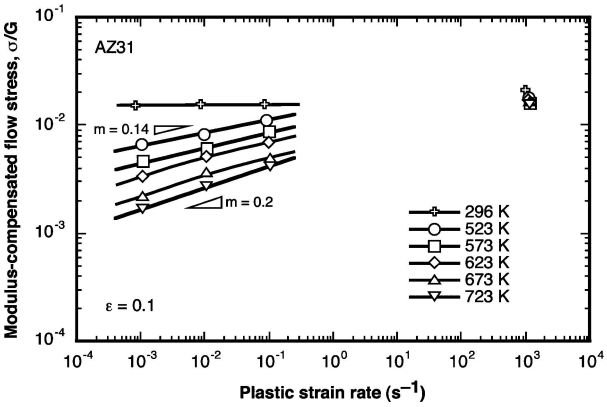

Figure 4 The variation in shear modulus compensated flow stress as a function of strain rate at various temperatures.

It is especially noted that the decrease in flow stress with temperature at strain rates below 10^{-1} s^{-1} was far greater than that at a strain rate of 10^{3} s^{-1}.

It is beneficial to examine the elastic modulus of the present material, since the temperature dependence of shear modulus is included in Fig. 2. The variation in shear modulus as a function of temperature of measurement is shown in Fig. 3. The shear modulus decreased linearly with increasing temperature. The temperature dependence of shear modulus, dG/dT, of the present material was calculated to be -0.0120 GPa K^{-1}, and was close to that of pure magnesium ($dG/dT = -0.0088$ GPa K^{-1}) [39].

The variation in modulus compensated flow stress, σ/G, as a function of true plastic strain rate is shown in Fig. 4. The shear modulus at 723 K was estimated by extrapolation. The slope of the curve in Fig. 4 indicates the strain rate sensitivity exponent, m. The m-value in the low strain rate range at room temperature was less than 0.01. The m-value at low strain rates below 10^{-1} s^{-1} increased with temperature and exhibited ~0.14 from 523 to 573 K, and ~0.2 from 673 to 723 K. Though the flow stress at a strain rate of 10^{3} s^{-1} decreased monotonically with temperature as has been shown in Fig. 2, the stress level was similar for all temperatures after compensation by temperature dependent shear modulus.

4. Discussion

4.1. High temperature deformation mechanism in the low strain rate range

In this section, high temperature deformation mechanism in the strain rate range between 10^{-3} to 10^{-1} s^{-1}

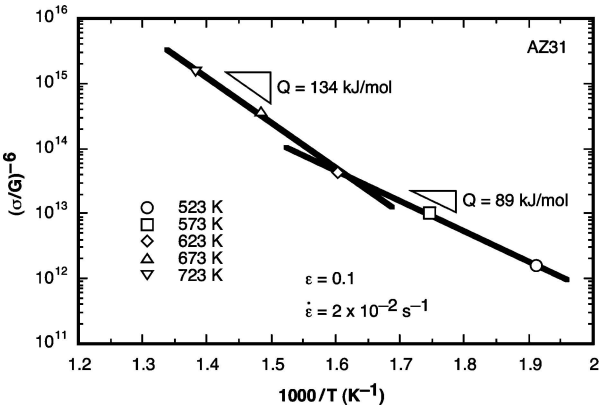

Figure 5 The variation in $(\sigma/G)^{-6}$ at fixed strain rate of 2×10^{-2} s^{-1} as a function of reciprocal temperature.

is discussed. The constitutive equation to describe the high temperature deformation is generally expressed as [40]

$$\dot{\varepsilon} = A\left(\frac{\sigma}{G}\right)^{n}\left(\frac{D_0}{b^2}\right)\exp\left(-\frac{Q}{RT}\right) \qquad (1)$$

where $\dot{\varepsilon}$ is the strain rate, A is a constant, σ is the flow stress, G is the shear modulus, n is the stress exponent ($=1/m$), D_0 is the pre-exponential factor for diffusion, b is the Burgers vector, R is the gas constant, T is the absolute temperature and Q is the activation energy for diffusion, which is dependent on the rate controlling process. The stress exponent, n, observed in the present material was 5–7 ($m = 0.14$–0.2) as has been shown in Fig. 4. The n-value of 5–7 suggests that climb controlled dislocation creep could be a dominant deformation process [41]. For simplicity, assuming that the stress exponent is 6, the relationship between $(\sigma/G)^{-6}$ and reciprocal temperature at a fixed strain rate of 2×10^{-2} s^{-1} is illustrated in Fig. 5. The activation energy can be calculated from the slope of the line in this figure. Inspection of the data in Fig. 5 reveals that the behaviors are divided into two regions. The activation energy value at 523–623 K is 89 kJ/mol, which is close to that for pipe diffusion of magnesium (92 kJ/mol) [39]. However, the activation energy at 623–723 K is 134 kJ/mol, which is close to that for lattice diffusion of magnesium (135 kJ/mol) [39]. It is suggested from the stress exponent and the activation energy that the dominant deformation mechanism in the present material is dislocation creep, which is controlled by pipe diffusion at low temperatures, and is controlled by lattice diffusion at high temperatures, respectively.

It was demonstrated from the experimental results that the dominant diffusion process varies with temperature in the present material. Robinson and Sherby [42] introduced the notion of an effective diffusivity involving the lattice diffusion coefficient, D_L, and pipe diffusion coefficient, D_p. The effective diffusion coefficient, D_{eff}, is given by [42, 43]

$$D_{eff} = D_L + \beta(\sigma/G)^2 D_p \qquad (2)$$

where β is a constant and is generally considered to be 7.4 for dislocation creep [43] when the relationship

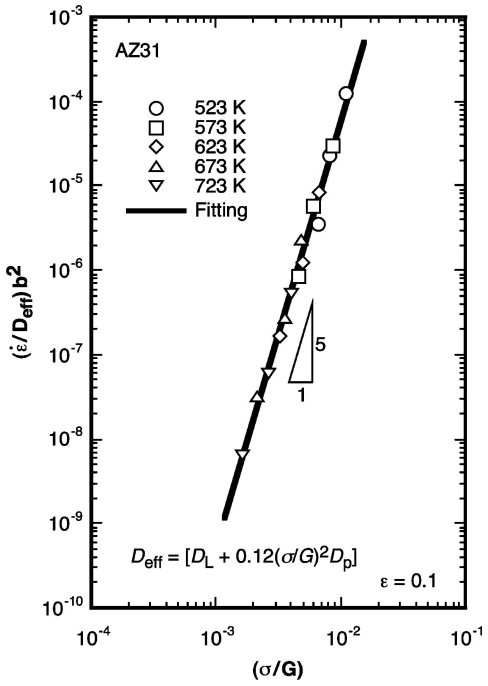

Figure 6 The variation in $(\dot{\varepsilon}/D_{eff})b^2$ as a function of (σ/G) in the low strain rate range.

is put into our format assuming that the Poisson's ratio, ν, is 0.3 [19]. Kim *et al.* [19] pointed out that the β-value is different in magnesium alloys with h.c.p. structure, and is estimated to be 0.12 for AZ31 and AZ61 magnesium alloys. In fact, it was demonstrated that this β-value can correctly predict the activation energy observed in the present material. The smaller β-value in magnesium alloys is believed to be related to the low dislocation density resulting from the limited slip systems in h.c.p. structure. Using $\beta = 0.12$, the variation in $(\varepsilon/D_{eff})b^2$ as a function of (σ/G) is shown in Fig. 6. The D_p and D_L for AZ31 was taken to be that for pure magnesium [39]. The pipe diffusion coefficient was assumed to be the same as the grain boundary diffusion coefficient [19, 43] in the present analysis, too. It is obviously noted that the deformation behavior in the present material is represented by a single straight line with a slope of 5 in the normalized plot compensated by effective diffusion coefficient, although the material showed different activation energy between high temperatures and low temperatures. Kim *et al.* [19] expected that the deformation behavior at temperatures higher than 700 K may not obey the same relation with that at lower temperatures, based on the results that extensive non-basal slip can occur at above this temperature [44]. However, the dislocation creep behavior observed in the present material was able to be represented by the same relation, at least, between 523 and 723 K.

4.2. Deformation mechanism at high strain rates

Temperature dependence of modulus-compensated flow stress at a strain rate of 10^3 s^{-1} is shown in Fig. 7 for the present AZ31. It is interesting to note that the stress level did not decrease with increasing temperature after

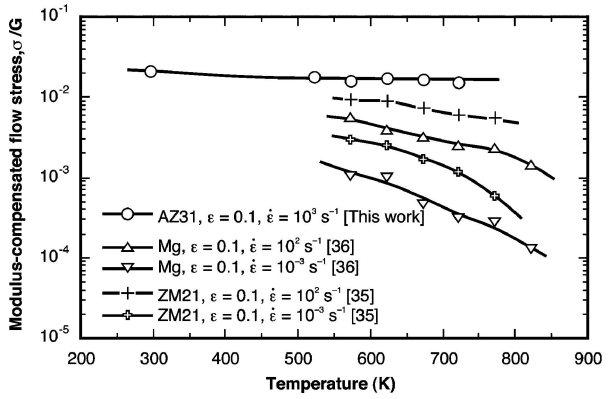

Figure 7 The variation in shear modulus compensated flow stress as a function of deformation temperature at a strain rate of 10^3 s^{-1} in AZ31 alloy. The data for pure magnesium [36] and ZM21 alloy [35] are also included.

compensation by temperature dependent shear modulus except at room temperature. The higher stress level at room temperature may be related to the extensive strain hardening as has been shown in Fig. 1b. Almost similar flow stress at elevated temperatures indicates that diffusion process is not a rate-controlling at a strain rate of 10^3 s^{-1}. It is concluded that the temperature dependence of flow stress at 10^3 s^{-1} is described only by the temperature dependence of shear modulus in the present material.

Mwembela *et al.* [34] and Beer *et al.* [37] investigated the high temperature deformation behavior of AZ31 at a strain rate of 1 s^{-1}. The analyses revealed that the flow behavior at 1 s^{-1} is still represented by a conventional creep equation, indicating that the diffusion contributes to the deformation. The deformation behavior at a relatively high strain rate of 10^2 s^{-1} has also been examined in pure magnesium [36] and Mg–Zn–Mn alloy, ZM21 [35]. The results are included in Fig. 7. The shear modulus for pure magnesium was taken from reference [39], and that for ZM21 alloy was assumed to be the same as the present material, AZ31. It is noted that the stress level at 10^2 s^{-1} decreased with temperature even after compensation by shear modulus for both materials. This may be explained by the significant strain hardening at low temperatures and/or the contribution of diffusion to the deformation.

Deformation mechanism map for pure magnesium with a grain size of 100 μm, which was constructed by Frost and Ashby [39], predicts that the plasticity by dislocation glide and by twinning dominates the deformation at high stress levels even at elevated temperatures, though no experimental data for high temperature deformation are presented. The upper stress level, below which power-law creep dominates the deformation in AZ31, is estimated to be, at least, $(\sigma/G) = 8 \times 10^{-3}$ to 1×10^{-2} from the literature [19, 34, 45] and from Fig. 6. It is noted that the stress level at a strain rate of 10^3 s^{-1} was always higher than the upper stress level for power-law creep in AZ31, indicating that the power law broke down completely at all temperatures examined. On the other hand, since the normalized stress for pure magnesium and ZM21 was lower than $(\sigma/G) = 10^{-2}$ at elevated temperatures, the decrease in flow stress with temperature may be resulting from the contribution by diffusion. The unusually temperature dependence of the flow stress at 10^3 s^{-1}, i.e., no temperature dependence of the normalized flow stress, is the first observation of this type in magnesium alloys.

In order to confirm the high temperature deformation mechanism at a high strain rate of 10^3 s^{-1}, deformed microstructures were inspected. The optical microstructures are shown in Fig. 8. The specimens were deformed at (a) $T = 296$ K, $\dot{\varepsilon} = 10^{-3}$ s^{-1}, (b) $T = 296$ K, $\dot{\varepsilon} = 10^3$ s^{-1}, (c) $T = 673$ K, $\dot{\varepsilon} = 10^{-3}$ s^{-1}, (d) $T = 673$ K, $\dot{\varepsilon} = 10^3$ s^{-1} and (e) the same condition as (d) but different region in the same specimen. The plastic strain is different among all materials. The specimens were deformed to the nominal strain of approximately -27 and -35% at 10^{-3} and 10^3 s^{-1}, respectively at room temperature, and approximately -55 and -23% at 10^{-3} and 10^3 s^{-1}, respectively at 673 K. The strain does not

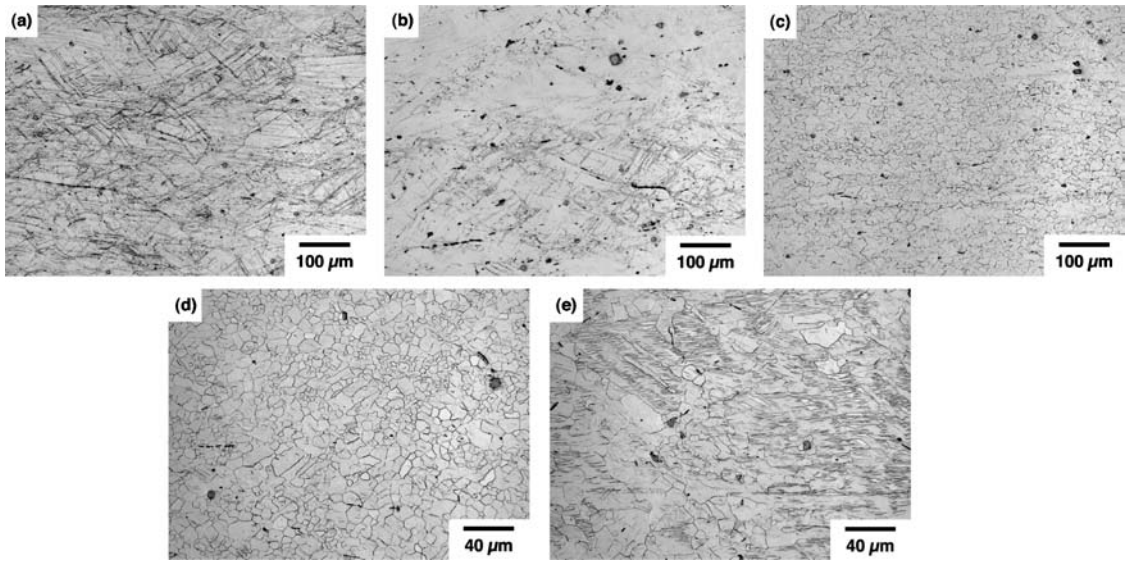

Figure 8 Optical microstructures after compression tests deformed at (a) $T = 296$ K, $\dot{\varepsilon} = 10^{-3}$ s^{-1}, (b) $T = 296$ K, $\dot{\varepsilon} = 10^3$ s^{-1}, (c) $T = 673$ K, $\dot{\varepsilon} = 10^{-3}$ s^{-1}, (d) $T = 673$ K, $\dot{\varepsilon} = 10^3$ s^{-1} and (e) same condition as (d) but different region in the same specimen. The compression direction is vertical.

correspond to the fracture strain except for deformation at $T = 296$ K, $\dot{\varepsilon} = 10^{-3}$ s^{-1}. As can be seen in Figs 8a and b, deformation twins were observed when the materials were deformed at room temperature. Highly dense deformation twins were formed in the material deformed at low strain rates when compared with that at a high strain rate. The fewer twins observed in the material deformed at 10^3 s^{-1} may be associated with the localization of the flow.

Mukai *et al*. [46] demonstrated in Mg–Zn–Zr alloy, ZK60, that the grain size dependence of the yield stress at room temperature obeys the Hall-Petch relation even at a high strain rate of 1.8×10^3 s^{-1}. This indicates that the deformation by slip still operates at high strain rates in magnesium alloys. Furthermore, deformation twins were also observed in coarse-grained materials. Because of the similarity in the deformed microstructure as well as significant strain hardening, the present AZ31 alloy may also deform by dislocation glide and twining at room temperature over a wide strain rate range.

When the materials were deformed at elevated temperatures and at low strain rates, equiaxed and finer grains were observed as shown in Fig. 8c, indicating that recrystallization took place during deformation. On the other hand, the microstructure was non-uniform when the material was deformed at 10^3 s^{-1}: completely recrystallized microstructure was observed in Fig. 8d, whereas regions containing many deformation twins were also remained in places as shown in Fig. 8e. The non-uniformity of the microstructure indicates that the deformation at 10^3 s^{-1} is still localized at 673 K as well as at room temperature. In general, domains of recrystallized grains and the deformation twins rarely coexist in AZ31 alloy deformed at relatively high temperatures at above 573 K irrespective of the processing routes (rolling, extrusion and forging) [12, 29, 47, 48]. The microstructure observed in the present material deformed at 10^3 s^{-1} is unique.

It has been pointed out that the recrystallized grain size and the deformation conditions can be correlated using the Zener–Hollomon parameter, Z [49], in magnesium alloys [50]. The variation in recrystallized grain size as a function of Z is shown in Fig. 9 for the present material deformed at a strain rate of 10^{-3} s^{-1} at temperatures ranging from 523 to 723 K, and at a strain rate of 10^3 s^{-1} at 673 K. The grain sizes were calculated only from the recrystallized region. The Z-parameter was calculated by $Z = \dot{\varepsilon} \exp(Q_L/RT)$ [50], where Q_L is the activation energy for lattice diffusion in pure magnesium [39]. The data by Chino *et al*. [30] for AZ31 alloy, that was deformed in compression at temperatures ranging from 473 to 673 K and at a strain rate of 4×10^{-3} s^{-1}, are also included in the figure. The recrystallized grain size of the present material deformed at 10^{-3} s^{-1} agreed well with the relation derived for reference data, except at 723 K. The deviation at 723 K is probably because the deformation temperature is higher than the temperature for solid solution treatment (=686 K). On the other hand, the recrystallized grain size of the present material deformed at 673 K and at 10^3 s^{-1} obviously deviated from the relation at low strain rates. This suggests that the recrystallization mechanism at $\dot{\varepsilon} = 10^3$ s^{-1} is different from that at $\dot{\varepsilon} = 10^{-3}$ s^{-1}. Recently, it was reported that the twin boundaries evolve into high angle boundaries by room temperature deformation of $\varepsilon \geq 0.5$ in pure magnesium [51–53]. Though the deformation conditions (temperature, strain, strain rate) and alloying additions differ from the present investigation, it is tempting to speculate that the similar recrystallization mechanism operates at 10^3 s^{-1} in AZ31, too, because the operating mechanism in the present material is expected to be dislocation glide and twinning. Supposing that the microstructural evolution occurs only at the flow localized region by the "twin dynamic recrystallization" [51–53], the recrystallized regions will be formed here, and the regions with deformation twins also remain where flow localization was less. In conclusion, in spite of the existence of the recrystallized grains, it is suggested that the present AZ31 alloy deforms by dislocation glide and twining at high strain rates of $\sim 10^3$ s^{-1}.

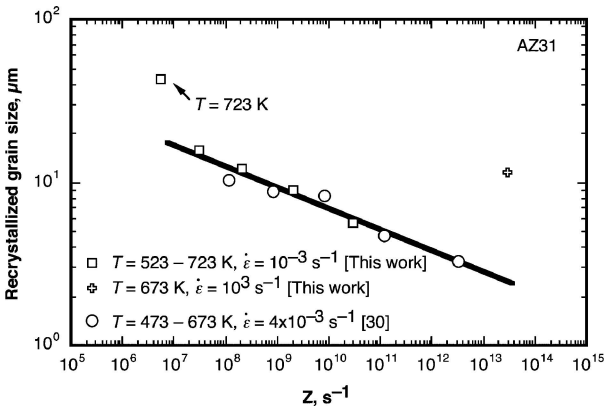

Figure 9 The variation in recrystallized grain size as a function of Z-parameter in AZ31.

5. Summary

High temperature compressive properties in AZ31 magnesium alloy were examined over a wide strain rate range from 10^{-3} to 10^3 s^{-1}. A special attention was paid to the deformation behavior and its mechanism at high strain rates of $\sim 10^3$ s^{-1}.

(1) In the low strain rate range below 10^{-1} s^{-1}, the strain rate was proportional to the five to seven power of stress. The activation energy was close to that for pipe diffusion at 523–623 K, and was close to that for lattice diffusion at 623–723 K. It was suggested that the dominant deformation mechanism in the low strain rate range was dislocation creep controlled by pipe diffusion at low temperatures, and by lattice diffusion at high temperatures. In spite of the different activation energy between high temperatures and low temperatures, the deformation behavior was represented by a single constitutive equation with a slope of 5 from 523 to 723 K by using effective diffusion coefficient.

(2) The flow stress at a high strain rate of 10^3 s^{-1} was not dependent on the deformation temperature after compensation by temperature dependent dynamic

shear modulus, indicating that the diffusion process is not a rate-controlling. Analysis of the flow behavior and microstructural observations indicated that the operating deformation mechanisms at high strain rates were dislocation glide and twinning even at elevated temperatures.

References

1. I. J. POLMEAR, *Mater. Sci. Tech.* **10** (1994) 1.
2. Y. TAKEBAYASHI and S. KOIKE, *Kobe Steel Eng. Reports* **47** (1997) 69.
3. F. H. FROES, D. ELIEZER and E. AGHION, *JOM* **50** (1998) 30.
4. F. VZERWINSKI, A. ZIELINSKA-LIPIEC, P. J. PINET and J. OVERBEEKE, *Acta Mater.* **49** (2001) 1225.
5. T. MUKAI, H. WATANABE, T. G. NIEH and K. HIGASHI, *Mat. Res. Symp. Proc.* **601** (2000) 291.
6. T. MUKAI, H. WATANABE and K. HIGASHI, *Mater. Sci. Forum* **350/351** (2000) 159.
7. R. E. REED-HILL and W. D. ROBERTSON, *Acta Metall.* **5** (1957) 728.
8. H. WATANABE, T. MUKAI, M. KOHZU, S. TANABE and K. HIGASHI, *Acta Mater.* **47** (1999) 3753.
9. H. WATANABE, T. MUKAI, M. MABUCHI and K. HIGASHI, *ibid.* **49** (2001) 2027.
10. T. SHIMIZU, *Alutopia* **31**(4) (2001) 41.
11. S. HAMA and F. WATANABE, *J. Japan Inst. Light Metals* **51** (2001) 514.
12. H. WATANABE, T. MUKAI, K. ISHIKAWA, Y. OKANDA, M. KOHZU and K. HIGASHI, *ibid.* **49** (1999) 401.
13. H. TAKUDA, H. FUJIMOTO and N. HATTA, *J. Mater. Process. Tech.* **80/81** (1998) 513.
14. J. KANEKO, M. SUGAMATA, M. NUMA, Y. NISHIKAWA and H. TAKADA, *J. Japan Inst. Metals* **64** (2000) 141.
15. J. KANEKO, T. ASAHINA, M. SUGAMATA, Y. NISHIKAWA and H. TAKADA, *ibid.* **64** (2000) 1239.
16. H. WATANABE, H. TSUTSUI, T. MUKAI, K. ISHIKAWA, Y. OKANDA, M. KOHZU and K. HIGASHI, *Mater. Sci. Forum* **350/351** (2000) 171.
17. H. SOMEKAWA, M. KOHZU, S. TANABE and K. HIGASHI, *ibid.* **350/351** (2000) 177.
18. H. WATANABE, T. TSUTSUI, T. MUKAI, M. KOHZU, S. TANABE and K. HIGASHI, *Int. J. Plasticity* **17** (2001) 387.
19. W.-J. KIM, S. W. CHUNG, C. S. CHUNG and D. KUM, *Acta Mater.* **49** (2001) 3337.
20. X. YANG, H. MIURA and T. SAKAI, *J. Japan Inst. Light Metals* **52** (2002) 318.
21. X. WU and Y. LIU, *Scripta Mater.* **46** (2002) 269.
22. H. K. LIN and J. C. HUANG, *Mater. Trans.* **43** (2002) 2424.
23. M. MABUCHI, Y. CHINO and H. IWASAKI, *ibid.* **44** (2003) 490.
24. H. WATANABE, T. MUKAI, K. SUZUKI and T. SHIMIZU, *J. Japan Inst. Light Metals* **53** (2003) 50.
25. H. NISHIMURA, O. HASEGAWA, N. KOISO and K. MATSUMOTO, *ibid.* **53** (2003) 302.
26. J. KOIKE, R. OHYAMA, T. KOBAYASHI, M. SUZUKI and K. MARUYAMA, *Mater. Trans.* **44** (2003) 445.
27. H. HOSOKAWA, Y. CHINO, K. SHIMOJIMA, Y. YAMADA, C. WEN, M. MABUCHI and H. IWASAKI, *ibid.* **44** (2003) 484.
28. H. SOMEKAWA, H. WATANABE, T. MUKAI and K. HIGASHI, *Scripta Mater.* **48** (2003) 1249.
29. H. WATANABE, H. TSUTSUI, T. MUKAI, K. ISHIKAWA, Y. OKANDA, M. KOHZU and K. HIGASHI, *Mater. Trans.* **42** (2001) 1200.
30. Y. CHINO, M. MABUCHI, K. SHIMOJIMA, Y. YAMADA, C. WEN, K. MIWA, M. NAKAMURA, T. ASAHINA, K. HIGASHI and T. AIZAWA, *ibid.* **42** (2001) 414.
31. E. DOEGE and K. DRÖDER, *J. Mater. Process. Tech.* **115** (2001) 14.
32. H. J. FROST and M. F. ASHBY, in "Deformation-Mechanism Maps" (Pergamon Press, Oxford, 1982) p. 153.
33. T. MUKAI, M. YAMANOI and K. HIGASHI, *Mater. Trans.* **42** (2001) 2652.
34. A. MWEMBELA, E. B. KONOPLEVA and H. J. MCQUEEN, *Scripta Mater.* **37** (1997) 1789.
35. "ASM Specialty Handbook, Magnesium and Magnesium Alloys," edited by M. M. Avedesian and H. Baker (AMS Int., Materials Park, OH, 1999) p. 278.
36. O. SIVAKESAVAM, I. S. RAO and Y. V. R. K. PRASAD, *Mater. Sci. Tech.* **9** (1993) 805.
37. A. G. BEER and M. R. BARNETT, in "Magnesium Technology 2002, Seattle," edited by H. I. Kaplan (TMS, Warrendale, PA, 2002) p. 193.
38. L. CISAR, Y. YOSHIDA, S. KAMADO, Y. KOJIMA and F. WATANABE, *Mater. Trans.* **44** (2003) 476.
39. H. J. FROST and M. F. ASHBY, "Deformation-Mechanism Maps" (Pergamon Press, Oxford, 1982) p. 43.
40. C. R. BARRET, A. J. ARDELL and O. D. SHERBY, *Trans AIME* **230** (1964) 200.
41. S.-E. HSU, G. R. EDWARDS and O. D. SHERBY, *Acta Metall.* **31** (1983) 763.
42. S. L. ROBINSON and O. D. SHERBY, *ibid.* **17** (1969) 109.
43. O. A. RUANO, J. WADSWORTH and O. D. SHERBY, *J. Mater. Sci.* **20** (1985) 3735.
44. S. S. VAGARALI and T. G. LANGDON, *Acta Metall.* **30** (1982) 1157.
45. S. W. CHUNG, H. WATANABE, W.-J. KIM and K. HIGASHI, *Mater. Trans.* **45** (2004) 1266.
46. T. MUKAI, M. YAMANOI, H. WATANABE, K. ISHIKAWA and K. HIGASHI, *ibid.* **42** (2001) 1177.
47. Y. CHINO, M. MABUCHI, R. KISHIHARA, H. HOSOKAWA, Y. YAMADA, C. WEN, K. SHIMOJIMA and H. IWASAKI, *ibid.* **43** (2002) 2554.
48. Y. YOSHIDA, L. CISAR, S. KAMADO and Y. KOJIMA, *ibid.* **44** (2003) 468.
49. C. ZENER and J. H. HOLLOMON, *J. Appl. Phys.* **15** (1944) 22.
50. M. MABUCHI, K. KUBOTA and K. HIGASHI, *Mater. Trans. JIM* **36** (1995) 1249.
51. R. KAIBYSHEV and O. SITDIKOV, *Z. Metallkd.* **85** (1994) 10.
52. R. O. KAIBYSHEV and O. S. SITDIKOV, *Phys. Met. Metall.* **89** (2000) 384.
53. O. STITDIKOV and R. KAIBYSHEV, *Mater. Trans.* **42** (2001) 1928.

Received 28 June
and accepted 8 November 2004